J Neuropathol Exp Neurol
Vol. 73, No. 9
September 2014
pp. 891–902

ORIGINAL ARTICLE

Neuropathology of the Anterior Midcingulate Cortex in Young Children With Autism

Neha Uppal, PhD, Bridget Wicinski, BS, Joseph D. Buxbaum, PhD, Helmut Heinsen, MD, Christoph Schmitz, MD, and Patrick R. Hof, MD

Abstract

The anterior cingulate cortex, which is involved in cognitive and affective functioning, is important in investigating disorders in which individuals exhibit impairments in higher-order functions. In this study, we examined the anterior midcingulate cortex (aMCC) at the cellular level in patients with autism and in controls. We focused our analysis on layer V of the aMCC because it contains von Economo neurons, specialized cells thought to be involved in emotional expression and focused attention. Using a stereologic approach, we determined whether there were neuropathologic changes in von Economo neuron number, pyramidal neuron number, or pyramidal neuron size between diagnostic groups. When the groups were subdivided into young children and adolescents, pyramidal neuron and von Economo neuron numbers positively correlated with autism severity in young children, as measured by the Autism Diagnostic Interview—Revised. Young children with autism also had significantly smaller pyramidal neurons than their matched controls. Because the aMCC is involved in decision-making during uncertain situations, decreased pyramidal neuron size may reflect a potential reduction in the functional connectivity of the aMCC.

Key Words: Anterior cingulate cortex, Anterior midcingulate cortex, Autism, Neuropathology, Stereology, von Economo neuron.

INTRODUCTION

Autism affects 1 in 68 children and is clinically defined by impairments in social communication and restricted and repetitive behaviors (1). Although causes of autism are slowly being identified, very few are common to even 1% of the affected population (2), and many have yet to be discovered. Although social and emotional impairments are well characterized and documented in autism, abnormalities in attention functioning, which likely subserves many high-order cognitive processes, are not yet well understood (3). One region that is involved in attention and cognitive control is the anterior cingulate cortex (ACC). The ACC integrates inputs from various sources, including sensory, motor, cognitive, and emotional information, to modulate value attribution, personality patterns, and social functioning (4, 5). The ACC is divided into 2 main areas: the ''affect'' area, encompassing Brodmann areas 24, 25, and 32, and the ''cognitive'' area, area 24′ (6). These regions have been parsed out according to their distinct projections and functions (7–9). The rostral segment of the ACC is involved in emotional behaviors and modulation of autonomic function, which is corroborated by significant inputs from the amygdala (10, 11), and outputs to the periaqueductal gray (5). The caudal segment of the ACC, defined as the midcingulate cortex (MCC) in the present study, is involved in control of skeletomotor function, response selection, nociceptive awareness, and executive control of attention (4, 5, 7, 12).

The MCC has been implicated in autism through its role in value attribution and reward (13) and consistently shows alterations in activity, as demonstrated by imaging studies (14–16). For instance, patients with autism exhibit reduced glucose metabolism, indicating reduced activity, throughout the anterior cingulate cortex and the posterior cingulate cortex (16). Diffusion tensor imaging studies also showed disrupted white matter in and adjacent to the ACC and MCC in patients with autism, suggesting impairments in connectivity (14). Reduced activity in the MCC was also shown to affect the attentional network in autism, with the lack of activity correlating with increased impairments in communication and language (15).

In parallel, the ACC has been assessed at the cellular level to uncover neuropathology that may represent the foundation of these functional changes. Kemper and Bauman (17) observed that patients with autism present with an unusually coarse and poorly laminated ACC in 5 of 6 cases. The first study to examine the ACC quantitatively analyzed the size and density of pyramidal neurons in the 3 subregions of the ACC (areas 24a, 24b, and 24c) according to the cytoarchitectural parcellation by Vogt et al (18), as well as von Economo neuron (VEN) density, size, and distribution in 9 male subjects with autism spanning

From the Fishberg Department of Neuroscience (NU, BW, PRH), Friedman Brain Institute (NU, BW, JDB, PRH), Seaver Autism Center for Research and Treatment (NU, JDB, PRH), Graduate School of Biomedical Sciences (NU, JDB, PRH), and Department of Psychiatry (JDB), Icahn School of Medicine at Mount Sinai, New York, New York; and Morphologic Brain Research Unit, Department of Psychiatry, University of Würzburg, Würzburg (HH); and Department of Neuroanatomy, Ludwig-Maximilians University of Munich, Munich (CS), Germany.

Send correspondence and reprint requests to: Patrick R. Hof, MD, Fishberg Department of Neuroscience, Icahn School of Medicine at Mount Sinai, One Gustave L. Levy Place, Box 1639, New York, NY 10029; E-mail: patrick.hof@mssm.edu

This work was supported by the Seaver Foundation (NU, JDB, PRH), Autism Speaks (Autism Celloidin Library, PRH), the James S. McDonnell Foundation (PRH), and the Simons Foundation (PRH, JDB).

The authors declare no conflicts of interest.

adolescence and adulthood (19). Neuron size was significantly smaller in superficial layers II and III and in deep layers V and VI in area 24b, and neuron density was reduced in deep layers in area 24c. Although other pathologic changes were reported in that study, they only applied to smaller subgroups of patients with autism and could not be categorized using typical characteristics such as age, sex, or autism severity (19). To understand these subtle changes better, we have re-evaluated the possible presence of changes in VEN numbers, pyramidal neuron number, and pyramidal neuron number size, and their relationship with the diagnosis of autism.

MATERIALS AND METHODS

Subjects

A total of 14 postmortem brains (1 hemisphere per case, except for 1 control subject, coded both C1 and C2, and 1 patient with autism, coded both A1 and A2, in which both hemispheres were available) were analyzed. Subjects consisted of 7 patients with autism (4 male subjects, with both hemispheres analyzed in 1 male, and 3 female subjects, aged 4–21 years) and 7 control subjects (2 male subjects, with both hemispheres analyzed in 1 male, and 5 female subjects, aged 4–20 years), making a total of 8 pairs. This work involved exclusively postmortem materials and was approved by Autism Speaks and the Icahn School of Medicine at Mount Sinai Institutional Review Board. All postmortem materials used in this study were directly obtained from Autism Speaks. All necessary written informed consent forms were obtained from the patients or their next of kin and confirmed at the time of death. Demographic and clinical characteristics of the series are summarized in Table 1.

Tissue Preparation

Tissue processing for all cases used in this study was performed at the New York State Institute for Basic Research in Developmental Disabilities (Staten Island, NY) and at the Morphologic Brain Research Unit, University of Würzburg (Würzburg, Germany), as described previously (20–22). Brains were divided mediosagittally, and either the left hemisphere or the right hemisphere was available for each case; in a select few cases, both hemispheres were processed. Immersion-fixation was performed in 10% formalin for at least 3 months, followed by embedding in celloidin and cutting into complete series of 200-μm-thick sections (every third section available for our analysis) or 500- and 600-μm-thick sections (every other section available for our analysis).

Regional Definition

The MCC encompasses several cytoarchitecturally and functionally distinct areas; in this study, we focused on the anterior MCC (aMCC). This region corresponds to the ACC domain investigated in a previous neuropathologic study of patients with autism (19). Our sampled sections ranged from the midline crossing of the genu of corpus callosum to the crossing of the anterior commissure, which encompasses the aMCC. Cytoarchitecturally, the aMCC corresponds to area 24′, as described by Vogt et al (18) (Figs. 1A, B). Area 24′ is localized in the midline surface of the brain, bordered ventrally by the callosomarginal area 33 and the corpus callosum and dorsally by paracingulate area 32′ (a cingulofrontal transition area). Anteriorly, area 24′ merges with area 24 (ACC); posteriorly, area 24′ borders area 23, the posterior cingulate cortex (18).

Area 24′ is an agranular cortex that is subdivided into 3 segments: areas 24a′, 24b′, and 24c′, with each of these subareas being adjacent in a ventrodorsal sequence (Figs. 1C–E). As defined by Vogt et al (18), area 24a′ has a well-defined laminar architecture, with clear layers II and III, a distinct layer Va populated with large neurons adjacent to a neuron-sparse layer Vb, and a denser layer VI populated with smaller neurons. Area 24b′ has a distinct layer II, broad layers III and Vb, and a robust layer Va with large pyramidal neurons. In area 24c′, layers II and III are as thick as or thicker than layers V and VI. A greater amount of smaller neurons in layer Va makes this layer more prominent, though thinner, in area 24c′ than in adjacent area 24b′; in addition, layer Vb in area 24c′ has more medium-sized neurons, making the subdivisions of layer V less distinguishable. This area is anterior to the posterior MCC, which abuts the posterior area 23.

Cytoarchitecturally, there are several defining features that clearly distinguish area 24′ from adjacent cortical regions (18). On its dorsal border, area 32′ has some characteristics of a frontal cortical area, with a clear layer IV and large neurons in layer IIIc, while still containing a prominent, though less dense, layer Va. On its ventral border, area 33 has little laminar distinction, with clear separation only between layers I and II, and a small population of large neurons distinguishing layer Va. Area 24 lies anterior to area 24′; both of these areas are subdivided into 3 segments (a, b, and c), but generally, area 24 has a higher neuron density and thicker layers III and Va (18). More specifically, area 24a has a less distinct layer II, a thinner layer III, a thicker layer Va, and a more clearly defined layer VI than area 24a′. Area 24b has thicker layers III and Vb compared with area 24b′, and area 24c has a denser layer III, but a more sparse layer Vb. Posteriorly, area 23 is a granular cortex with clear layers IIIc, IV, and Va.

Another prominent cytoarchitectural characteristic that defines both areas 24 and 24′ is the presence of VENs in layer Vb. These bipolar cells with symmetric basal and apical dendrites (Fig. 2C) are generally perpendicular to the pial surface and are observed in clusters of 2 to 3 VENs (23). Von Economo neurons are predominant in areas 24a′ and 24b′ and rarer in area 24c′ and have a clear rostrocaudal gradient; therefore, VENs are more prevalent in areas 24a and 24b than in areas 24a′ and 24b′ and are not present at all in area 23. Most VENs assessed were present in area 24b′, with a high density at the edges of area 24b′ (23). In some cases, a dimple was present in area 24b′, within which VENs were less common (23).

We considered these cytoarchitectural characteristics to be reliable criteria for defining the aMCC, in accordance with recent ACC parcellations (18, 23) and classic descriptions, including Brodmann area 24 and von Economo limbic anterior area (24, 25).

Stereologic Design

For stereologic quantification, within the anatomic range defined previously, we selected every fifth section in the

TABLE 1. Demographic and Clinical Data of Patients With Autism and Controls

Case	Diagnosis	Age, years	Sex	Hemisphere	Cut/ Mounted Thickness, μm	Postmortem Interval, hours	Brain Weight, g	Cause of Death	Relevant Clinical Information	ADI-R
425–02	A1	4	M	L	200/164.15	30	1,160	Drowning	–Symptoms present at 2 years –Frequent tantrums and self-injurious behavior –Used parents' hand to reach objects, echolalia, tendency to walk on his tiptoes –Stereotypic play	14, 10 (NV), 3
15-763-95	C1	4	M	L	600/515.14	3	1,380	Myocardial infarct	–No known disorder	—
425-02	A2	4	M	R	200/158.8	30	1,160	Drowning	–Symptoms present at 2 years –Frequent tantrums and self-injurious behavior –Used parents' hand to reach objects, echolalia, tendency to walk on his tiptoes –Stereotypic play	14, 10 (NV), 3
15-763-95	C2	4	M	R	600/567.9	3	1,380	Myocardial infarct	–No known disorder	—
443-02	A3	5	F	R	200/184.15	13.25	1,390	Multiple injuries	–Symptoms present at 18 months –Tendency to bump into people and objects, echolalia, used parents hands as tools, walked on tiptoes often –Chronic otitis media	26, 11 (NV), 4
426-02	C3	4	F	R	200/171.05	21	1,222	Lymphocytic myocarditis	–No known disorder	—
M6-06	A4	7	M	R	200/176.0	25	1,610	Drowning	–Regression after first seizure at 14 months –No spontaneous meaningful language –Used parents' hands as tools –No reciprocal social smiling or eye contact –Stereotypic play –Psychiatric and developmental disorders on maternal side	29, 14 (NV), 3
15-138-97	C4	7	F	R	500/372.67	74	1,350	Asthma	–No known disorder	—
M5-03	A5	8	M	R	200/176.7	22.2	1,570	Rhabdomyosarcoma	–Symptoms present at 3 years –Engaged in repetitive play, jumping up and down on tiptoes, echolalia –Cancer diagnosis at age 6 years –Abnormal EEG	19, 14 (V), 4
M3-04	C5	8	F	R	200/184.41	20	1,222	Multiple injuries	–No known disorder	—
445-02	A6	13	M	L	200/158.47	8	1,470	Seizure	–Seizures beginning at age 2 years –Language delays reported at 15 months –Occasionally engaged in arm flapping, head banging	28, 12 (NV), 3

									–Social disorders in immediate family	
M9-03	C6	14	M	R	200/167.66	20	1,464	Electrocution	–No known disorder	—
M5-05	A7	17	F	L	200/130.23	25	1,580	Dilated cardiomyopathy	–Abnormal reciprocal social interaction	15, 16 (V), 7
									–Responded socially appropriately with family, but not non–family members	
M16-06	C7	15	F	R	200/175.79	9	1,250	Multiple injuries	–No known disorder	—
M1-03	A8	21	F	R	200/235.55	50	1,108	Chronic obstructive pulmonary disease	–Oxygen deprivation at birth	21, 11 (NV), 7
									–Delayed motor milestones	
									–Regression after grand mal seizure at ages 5, 10, and 20 years	
									–Comorbidities (ADHD, epilepsy, microcephaly, schizophrenia)	
M1-07	C8	20	F	R	200/183.72	9	1,340	Multiple injuries	–No known disorder	—

Autism Diagnostic Interview—Revised scores are listed as qualitative abnormalities in reciprocal social interaction, qualitative abnormalities in communication (V and NV), and restricted, repetitive, and stereotyped patterns of behavior, respectively. Cutoff scores for autism are 10, 8 (V) or 7 (NV), and 3 in the order listed previously.
ADHD, attention deficit–hyperactivity disorder; EEG, electroencephalogram; F, female; L, left; M, male; NV, nonverbal; R, right; V, verbal.

200-μm-thick series and every third section in the 500- and 600-μm-thick series. This approach ensured that the aMCC was sampled in a consistent and unbiased manner. All quantitative analyses were performed using a stereology workstation equipped with a Zeiss Imager A1 microscope, Plan-Neofluar objectives 2.5× (numeric aperture, 0.075) and 40× (numeric aperture, 0.75) and Plan-Apochromat objective 63× (numeric aperture, 1.4 oil differential interference contrast), a motorized stage (Ludl Electronics, Hawthorne, NY), an MBF CX9000 camera (MBF Bioscience, Williston, VT), and stereology software (Stereo Investigator, version 11.01; MBF Bioscience). Intrarater quality control tests, although not performed directly for this set of analyses, were done independently of this study and in the same materials as part of a general pilot experiment to establish parameters and were found to be highly reliable.

Starting with a random section number, a systematic-random scheme was applied, sampling throughout the aMCC. The boundaries of layer V of the aMCC were traced at 2.5× using cytoarchitectural characteristics described previously. Given that VENs account for a very small percentage of the total neuron population in layer V with a nonhomogeneous distribution, we performed an exhaustive count in the x and y axes to ensure that every VEN had an equal probability of being counted (Table 2). A final estimate of the VEN population was done using the optical fractionator probe to account for the z

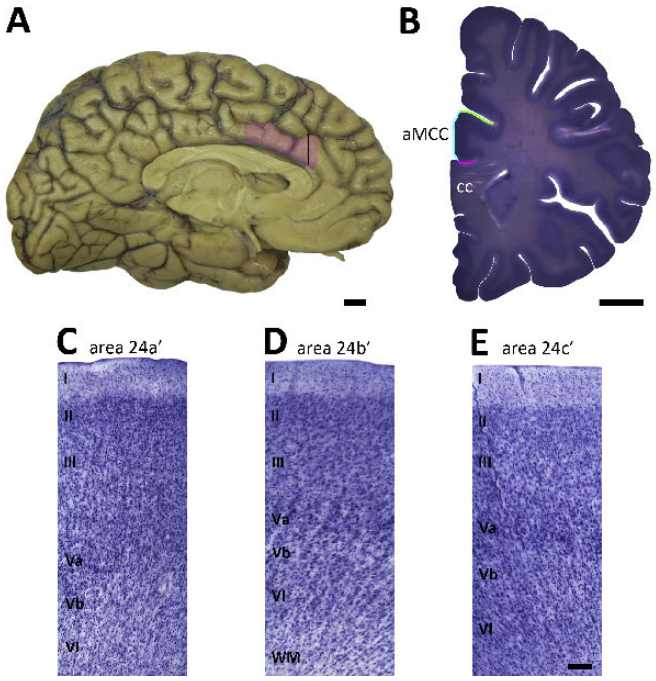

FIGURE 1. Cytoarchitectural characteristics of the aMCC. **(A)** Midsagittal view of the human brain depicting the location of the sampled aMCC in pink. **(B)** Nissl-stained section of the right hemisphere of a human brain showing the localization of the aMCC and outlining the individual subsections (area 24a′, pink; area 24b′, blue; area 24c′, green). Photomicrographs illustrating the cytoarchitectural characteristics of the subdivisions of area 24′ (the aMCC): area 24a′ **(C)**, area 24b′ **(D)**, and area 24c′ **(E)**. Scale bars = **(A, B)** 1 cm; **(C–E)** 200 μm. cc, corpus callosum.

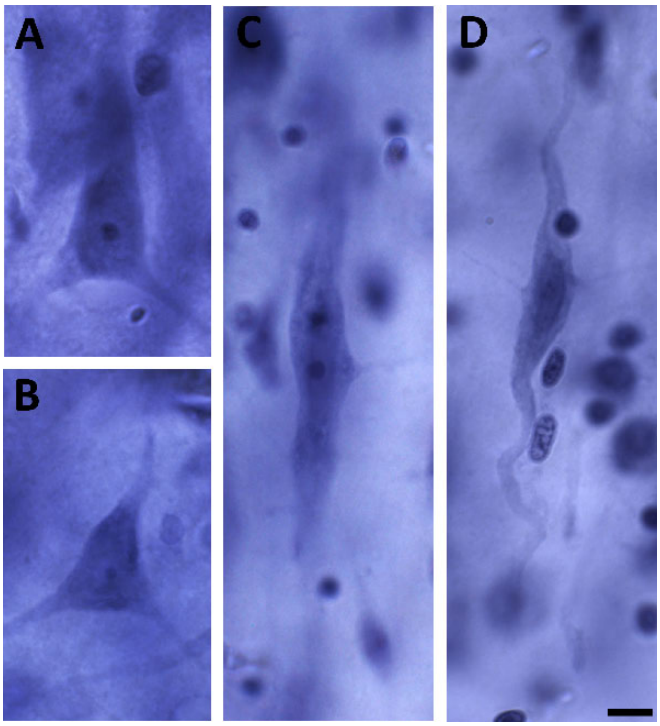

FIGURE 2. Pyramidal neurons and VENs in autism. **(A–D)** Photomicrographs showing the typical size and morphology of a pyramidal neuron **(A)** and the reduced pyramidal neuron size in a patient with autism **(B)**. A typical VEN in a control subject **(C)** and a VEN in a patient with autism **(D)**; note the atypical ''corkscrew'' morphology of the dendrites in **(D)**. Scale bar = 10 μm.

axis, given that disectors only sampled a fraction of the total thickness of the sections to avoid artifacts due inhomogeneous staining (26, 27). The mean measured thickness was calculated for each case before sampling using the 40× objective (at least 3 measured sites per section counted), and neurons were counted using the 63× objective. For a summary of the parameters used for the optical fractionator probe in the analysis of VENs and pyramidal neurons, see Table 2.

Neurons were identified as pyramidal neurons or VENs by their morphologic characteristics (Figs. 2A, C, respectively) (23, 28–31). Neurons were identified as VENs if they were present in layer V in the aMCC, were oriented perpendicularly to the pial surface, and presented a bipolar elongated shape with prominent dendrites emerging from apical and basal poles. Their staining was characteristically lighter than that of adjacent pyramidal neurons (23, 28–31). Pyramidal neurons were identified by their characteristic triangular morphology (dark and recognizable nucleoli, a large soma, and a visible apical dendrite), with several dendrites emerging from the basal surface. The pyramidal neuron population in layer V was estimated using the optical fractionator probe in the same sections used for VEN quantification. The dimensions of the sampling grid were set to sample enough pyramidal neurons such that the coefficient of error was 0.1 or less (26). Stereo Investigator defined a systematic-random sampling sequence of counting frames within the user-defined outline of layer V, in which pyramidal neurons were quantified (Table 2). Pyramidal neuron perikaryal volume was estimated with the nucleator probe (32) for every pyramidal neuron counted. Because of the typical shape of the pyramidal neurons and the 2-dimensional volume estimation calculation by the nucleator probe, we chose to use 4 rays to estimate neuron shape.

For both VEN and pyramidal neuron counts, 5-μm guard zones were used on the top and bottom of every section to prevent biases related to sectioning artifacts (26). The ratio of VENs to pyramidal neurons was calculated for each subject, and the total volume of layer V was estimated using the Cavalieri principle and corrected for overprojection (26).

Statistical Analysis

Paired *t*-tests were performed to compare the 8 autism patients and their age-matched controls. Measures of VEN number, pyramidal neuron number, ratio of VENs to pyramidal neurons, pyramidal neuron size, and layer V volume were all analyzed. In addition, correlations between these parameters and Autism Diagnostic Interview—Revised (ADI-R) scores were analyzed using linear regression analysis. We also used repeated-measures analysis of variance to control for potential effects of age, sex, postmortem interval, and hemisphere. In addition, because pairs 1 and 2 consisted of both hemispheres of the same patient with autism and a control, we also conducted paired *t*-tests excluding each pair to determine whether having both hemispheres of the same cases would confound the results. In all analyses, the criterion for statistical significance was a value of $p = 0.05$ for a 2-sided test. Calculations were performed using GraphPad Prism version 5.03 (GraphPad Software, San Diego, CA).

Photography

The photograph of the full brain in Figure 1A was taken with a Nikon Coolpix P100 and produced with Adobe Photoshop version 11.0.2 (Adobe Systems Inc, San Jose, CA). Figure 1B was generated by scanning a histologic section of the right hemisphere of the brain of Case C4 at high resolution (1,200 dpi; CanoScan LiDE 500F Scanner; Canon, Tokyo, Japan). The photomicrographs used in Figures 1C to E are photomicrographs of Case C7 taken at 20× of subareas in the aMCC. Photomicrographs of individual pyramidal neurons in

TABLE 2. Stereologic Parameters Used for Quantification in Control Subjects and Patients With Autism

Parameters Assessed	VENs	Pyramidal Neurons
No. sections, mean	6.9	6.9
Objective 1	2.5×	2.5×
Objective 2	63×	63×
Disector height, μm	20	20
Guard zone, μm	5	5
Counting frame, μm	140 × 110	50 × 50
Grid, μm	140 × 110	650 × 400
Measured thickness, mean, μm		
Cut at 200 μm	174.36	174.36
Cut at 500 μm	372.67	372.67
Cut at 600 μm	541.52	541.52
Schmitz-Hof coefficient of error (mean, 26)	0.049	0.073

Figure 2 were taken with the 63× objective. All images were edited for brightness and contrast in Adobe Photoshop without altering the appearance of the original materials. Graphs in Figures 3 through 6 were created using GraphPad Prism version 5.03 (GraphPad Software).

RESULTS

This study focused on layer V of the aMCC, located in the midline, dorsal to the corpus callosum. The aMCC roughly begins along with the anterior aspect of the crossing of the genu and continues posteriorly until the level of the crossing of the anterior commissure. This area is of particular interest because of the presence of many VENs in layer V. Therefore, we estimated VEN number, pyramidal neuron number, pyramidal neuron size, and layer volume in patients with autism and in control subjects to understand whether VENs were selectively disrupted in autism.

Analyses included all pairs listed in Table 1. The estimated mean VEN population (t_7 = 1.042, p = 0.332) was not significantly different between patients with autism and controls, nor was the mean pyramidal neuron number (t_7 = 0.023, p = 0.983) or the mean ratio of VENs to pyramidal neurons (t_7 = 0.877, p = 0.41; Fig. 3A). There was no difference in mean perikaryal volume (t_7 = 1.506, p = 0.176), mean density of VENs (t_7 = 0.561, p = 0.593), mean density of pyramidal neurons (t_7 = 0.662, p = 0.529), and mean volume of layer V (t_7 = 0.756, p = 0.475) between patients with autism and controls (Fig. 3B). Full results are shown in Table 3. These results were still nonsignificant when either pair 1 or pair 2 was removed from the analysis (Table 4).

We also assessed each parameter with repeated-measures analysis of variance to control for age, postmortem interval, sex, and hemisphere. All parameters, except perikaryal volume, were not significantly affected by these covariates. As was age (F_1 = 27.552, p = 0.002), sex was a significant covariate with perikaryal volume, with male subjects having larger neurons than female subjects (F_1 = 6.548, p = 0.043) (Fig. 4). To further explore this age effect on perikaryal volume, we subdivided the autism and control groups into young children (aged 4–8 years) and adolescents (aged 13–21 years) to determine if there were age-specific changes. When statistical analyses were performed for these groups in all analyzed parameters, young children with autism were found to have significantly smaller mean perikaryal volume than controls on paired *t*-test (t_4 = 4.378, p = 0.012) and unpaired *t*-test (t_8 = 4.496, p = 0.002) (Fig. 5). Young control children had significantly higher perikaryal volumes than control adolescents (t_6 = 3.287, p = 0.017, unpaired *t*-test), whereas adolescents with autism had significantly higher mean perikaryal volumes than young children with autism (t_6 = 3.683, p = 0.01, unpaired *t*-test; Fig. 5). These results also remained significant when pair 1 or pair 2 was excluded (Table 4).

To determine whether the analyzed parameters correlated with ADI-R scores, we performed linear regression for each parameter with each ADI-R score. The ADI-R is a quantitative index of autism severity, as assessed through the 3 major characteristics of autism: impairments in social interaction, impairments in social communication, and presence of restrictive and repetitive behaviors. These behaviors are measured on a scale, with higher scores corresponding to

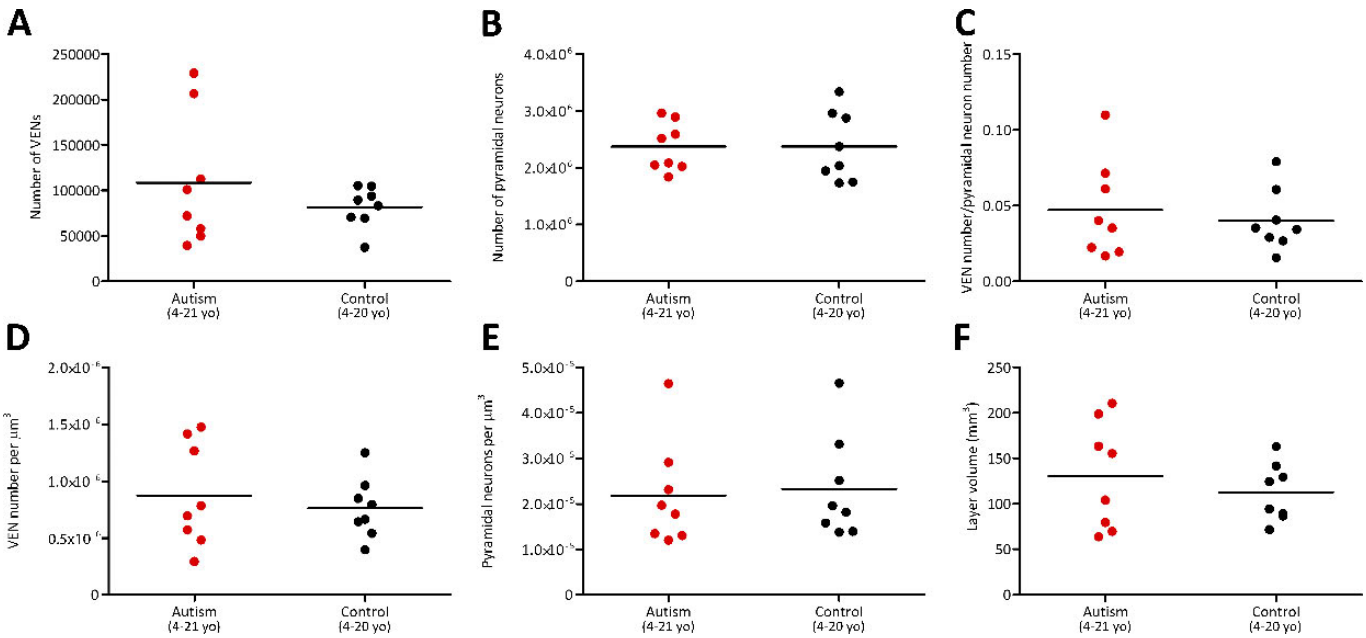

FIGURE 3. Neuron numbers and densities are not significantly different in patients with autism and in controls. Typically developing controls are shown in black, and patients with autism are shown in red. There is no significant difference in the estimated population of VENs **(A)**, the estimated population of pyramidal neurons **(B)**, or the ratio of VENs to pyramidal neurons **(C)** in patients with autism and in controls. There is also no significant difference in VEN density **(D)**, pyramidal neuron density **(E)**, or layer volume **(F)**.

TABLE 3. Summary of Stereologic Quantification for All Parameters in Patients With Autism and in Controls

Case	Ratio of VENs to Pyramidal Neurons	Estimated VEN Population	Estimated Pyramidal Neuron Population	Perikaryal Volume, μm^3	Layer V Volume, mm^3	Density of VENs	Density of Pyramidal Neurons
A1	0.0353	72,267	2,047,607	2,007	104.08	6.94328×10^{-7}	1.9673×10^{-5}
A2	0.0612	112,549	1,839,380	1,712	79.56	1.41461×10^{-6}	2.31188×10^{-5}
A3	0.0714	206,616	2,893,733	1,965	163.31	1.26518×10^{-6}	1.77193×10^{-5}
A4	0.1098	229,001	2,085,449	1,930	155.37	1.47391×10^{-6}	1.34225×10^{-5}
A5	0.0402	101,249	2,519,035	1,888	210.44	4.81139×10^{-7}	1.19706×10^{-5}
A6	0.0224	58,118	2,592,886	2,485	198.87	2.92217×10^{-7}	1.3037×10^{-5}
A7	0.0196	39,752	2,025,336	2,203	69.6	5.71167×10^{-7}	2.91×10^{-5}
A8	0.0168	49,879	2,961,382	2,145	63.75	7.82465×10^{-7}	4.6456×10^{-5}
A	0.0471 ± 0.113	108,679 ± 25,435	2,370,601 ± 151,255	2,042 ± 83*	130.6 ± 20.8	$8.719 \times 10^{-7} \pm 1.598 \times 10^{-7}$	$2.181 \times 10^{-5} \pm 4.07 \times 10^{-6}$
C1	0.0607	105,397	1,735,815	3,457	124.46	8.46807×10^{-7}	1.39463×10^{-5}
C2	0.0353	104,675	2,958,713	3,092	163.04	6.42005×10^{-7}	1.81467×10^{-5}
C3	0.0343	69,788	2,036,692	2,254	129.26	5.39921×10^{-7}	1.5757×10^{-5}
C4	0.079	93,801	1,943,995	2,645	141.56	6.62647×10^{-7}	1.37331×10^{-5}
C5	0.0405	70,813	1,747,653	2,774	89.25	7.93387×10^{-7}	1.95807×10^{-5}
C6	0.0157	37,346	2,376,580	2,212	94.31	3.95992×10^{-7}	2.51997×10^{-5}
C7	0.029	83,214	2,873,902	1,657	86.65	9.60302×10^{-7}	3.31653×10^{-5}
C8	0.0268	89,550	3,337,200	1,661	71.72	1.24854×10^{-6}	4.65284×10^{-5}
C	0.0402 ± 0.0072	81,823 ± 7,936	2,376,319 ± 216,208	2,470 ± 228*	112.5 ± 11.2	$7.612 \times 10^{-7} \pm 9.371 \times 10^{-8}$	$2.326 \times 10^{-5} \pm 3.282 \times 10^{-5}$

Rows "A" and "C" indicate the mean ± SE of the autism and control groups, respectively.
* $p < 0.05$.

increased severity of changes for a given behavior. The number of VENs was significantly positively correlated with social interaction score ($p = 0.0143$, $R^2 = 0.08981$), and the number of pyramidal neurons was significantly positively correlated with restricted and repetitive behavior scores ($p = 0.0249$, $R^2 = 0.8537$) (Fig. 6).

DISCUSSION

This study sought to assess whether neuropathology was present in the aMCC of children and adolescents with autism. Reduced pyramidal neuron size was found specifically in children with autism aged 4 to 8 years, with no changes in pyramidal neuron number and density, VEN number and density, or layer volume. No statistically significant difference was observed for all parameters when we compared adolescents with autism and their matched controls.

Potential Role of the aMCC in Autism

The aMCC is activated during acute nociceptive awareness, anxiety, pain anticipation, and reward (33–41), with inputs from the amygdala, insula, striatum, spinothalamic tract, inferior parietal cortex, and midline and intralaminar thalamic nuclei influencing its function (11, 42–50). Essentially, the aMCC seems to be involved in determining the optimal response to an uncertain situation by integrating information on punishment (and, potentially, information on reward) to send control signals to motor areas both cortically and subcortically (38, 51–53). In this scheme, each area connected to the aMCC

TABLE 4. Summary of Statistical Results in Patients With Autism and in Controls

Variable	p Value All Pairs	Without Pair 1	Without Pair 2
Ratio of VENs to pyramidal neurons	0.41	0.17	0.64
Estimated VEN population	0.332	0.254	0.356
Estimated pyramidal neuron population	0.983	0.865	0.527
Perikaryal volume, μm^3	0.176	0.355	0.35
Layer V volume, mm^3	0.475	0.414	0.189
Density of VENs	0.593	0.532	0.938
Density of pyramidal neurons	0.529	0.31	0.342
Perikaryal volume, μm^3			
Children aged 4–8 years	0.012	0.036	0.04
Autism	0.01	0.014	0.016
Controls	0.017	0.022	0.038

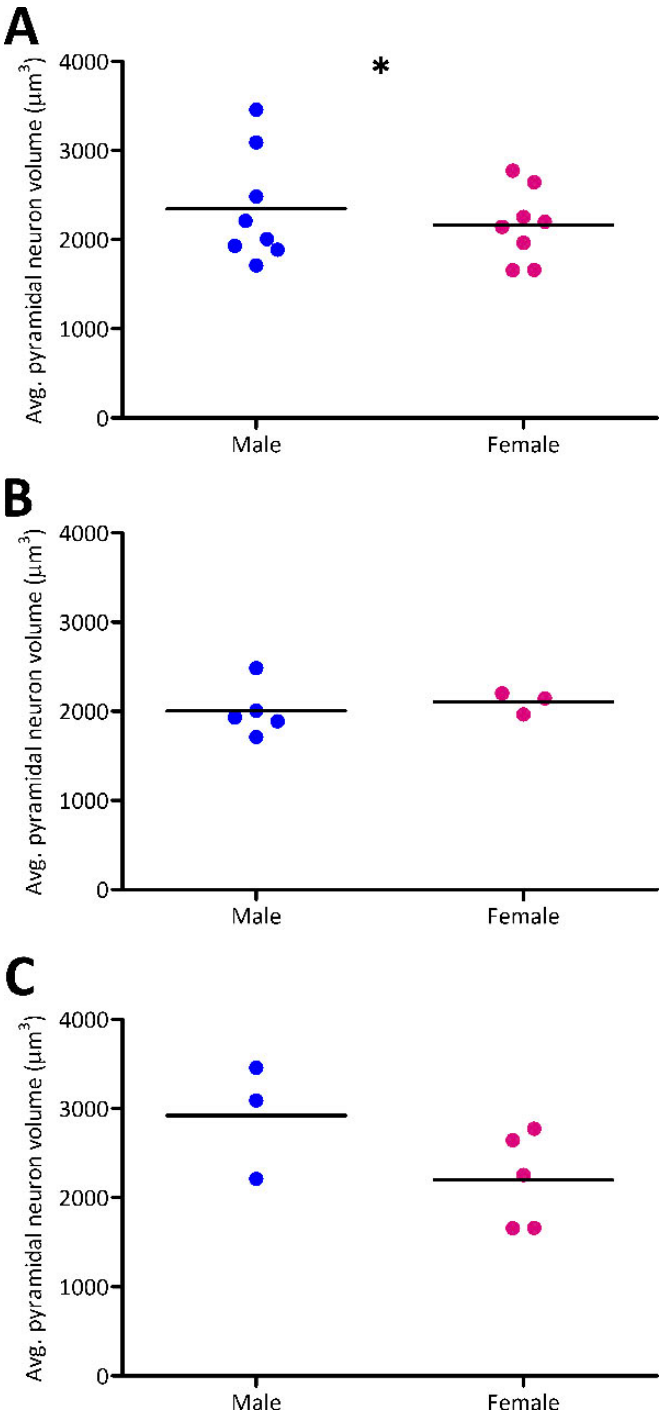

FIGURE 4. Sex differences in perikaryal volume. **(A)** Neuronal size in patients with autism and in controls is significantly larger in male subjects than in female subjects (* p = 0.043). **(B, C)** Sex differences between patients with autism **(B)** and controls **(C)**. Male subjects are shown in blue, and female subjects are shown in pink.

would play a specific role: Connections between the aMCC and the amygdala, for example, are likely crucial in influencing the activity of the aMCC, as the amygdala detects biologically salient stimuli for response formation, in addition to its well-documented role in fear and anxiety (54, 55).

A defining feature of children with autism is their propensity for routine; change, even in small quantities, is difficult to adjust to (56, 57). When change does occur, typically developing children can assess the current situation, weigh out courses of action, and respond promptly to achieve an optimal outcome. In situations that are not only uncertain but potentially threatening, the aMCC integrates the appropriate cognitive, affective, and noxious inputs to determine a suitable behavior. However, if the aMCC is functionally deficient, it can be challenging to handle a new, uncertain situation. Dysfunction of the aMCC may substantiate the feeling of uncertainty if the circuitry required to generate an adequate reaction to an uncertain situation is not properly established (38, 58).

Pyramidal Neurons in the aMCC

It may be the case that, in young children with autism, long-range connections among areas that interact with the aMCC to provide initial information on the current situation and consequences of relative courses of action are not communicating properly. In addition, these long-range connections between the aMCC and the appropriate motor-related areas are needed to act upon the planned response. These connections originate from pyramidal neurons, the main excitatory projection neurons in the cortex, and potentially from VENs. In the aMCC, young children with autism have significantly smaller layer V pyramidal neurons compared with controls. If there is a significant reduction in the size of pyramidal neurons, there could be a proportional effect on dendritic complexity and axonal length (59–62) and functional impairments at the cellular level (63–65), suggesting that inputs and outputs of the aMCC may not be adequately established. In fact, aMCC layer V pyramidal neurons are connected to cortical areas such as the insula and inferior parietal cortex, and subcortical areas, including the amygdala, striatum, and thalamus, have inputs to and/or outputs from the aMCC (11, 42–50). Impaired communication between these areas and the aMCC caused by neuropathologic changes in pyramidal neuron size and structure may thus represent a correlate of abnormalities in connectivity in young children with autism; this hypothesis is corroborated by white matter reduction in autism, as demonstrated in imaging studies (14, 66, 67).

Upon assessment of the developmental trajectory of pyramidal neurons in the aMCC, controls display a clear downward trend, with significantly larger pyramidal neurons in young children compared with adolescents (Fig. 5). This implies that pyramidal neurons display a smaller size with age, likely because of synaptic pruning (68). This same developmental trajectory goes slightly upward in patients with autism, as young children with autism have significantly smaller pyramidal neurons than their adolescent counterparts. This trend may reflect a delay in the development of certain connections from childhood to adolescence. In addition, the segregation of pyramidal neuron size by sex (Fig. 4) is an interesting finding, raising the possibility of sex differences in pathology severity. This finding should be considered with caution as the sample size is quite small.

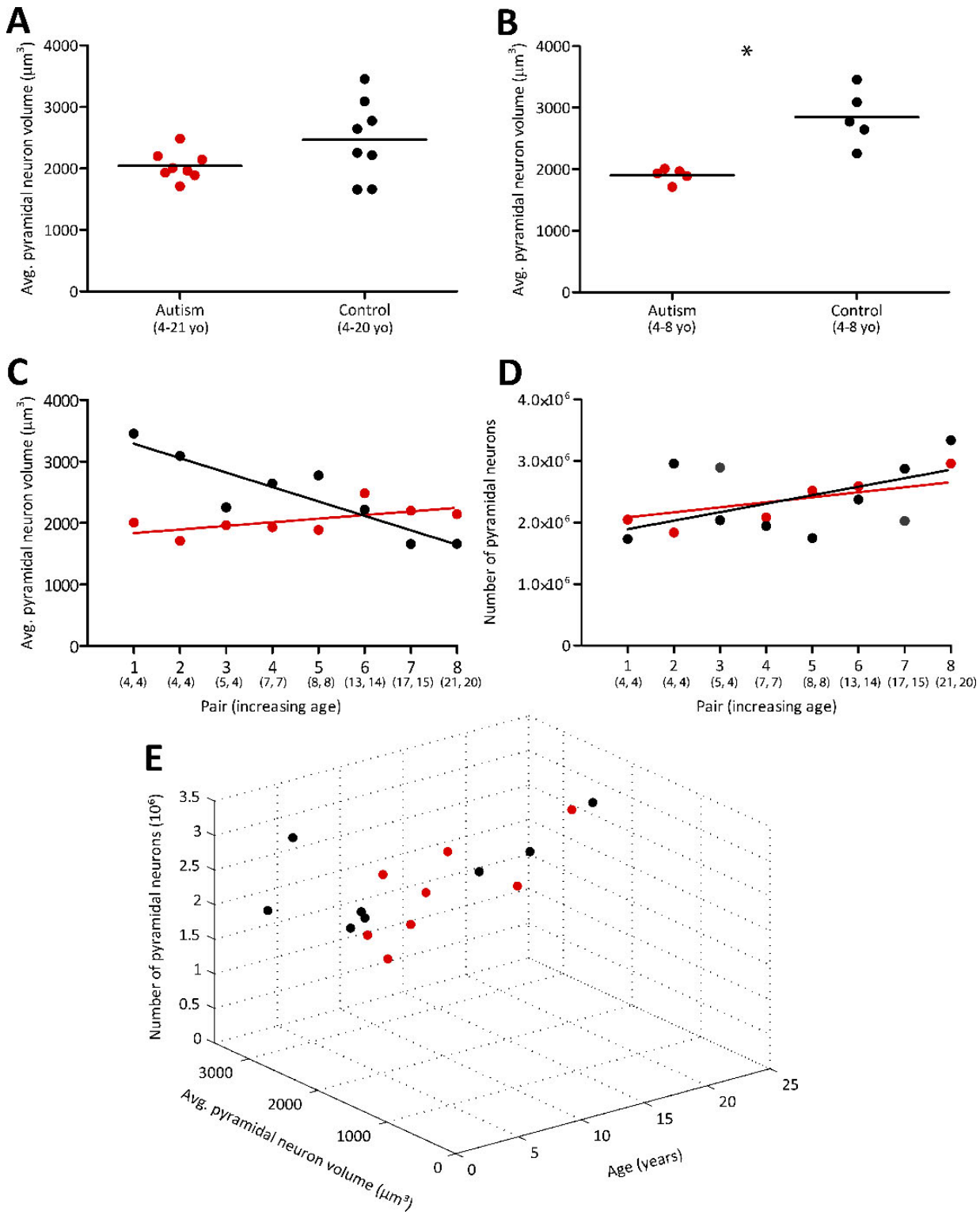

FIGURE 5. Perikaryal volume is significantly smaller in children with autism. **(A)** Neuronal size in patients with autism and in controls across all ages; note that the volume is not significantly different. **(B)** There is a significantly smaller size of neurons in children with autism (aged 4–8 years) versus age-matched controls (* p = 0.012). **(C)** Developmental trajectory of pyramidal neuron size in children and adolescents. **(D)** Developmental trajectory of pyramidal neuron number in children and adolescents. Ages of patients with autism and controls, respectively, are listed under each pair. **(E)** Three-dimensional graph depicting the relationship between pyramidal neuron number and volume with age. Typically developing controls are shown in black, and patients with autism are shown in red.

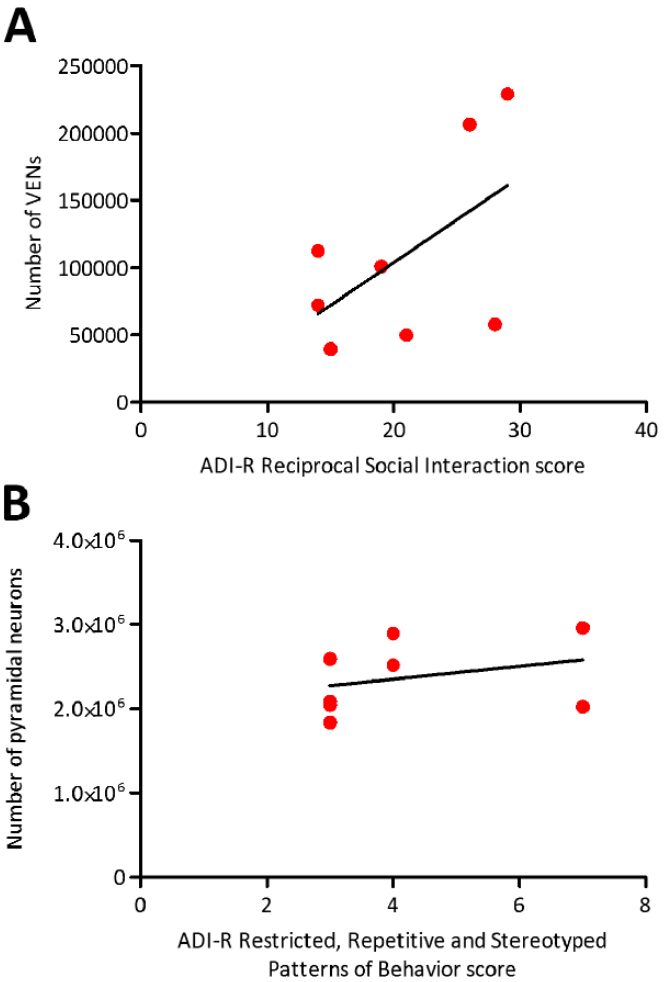

FIGURE 6. Autism Diagnostic Interview—Revised scores correlate with neuron number in children with autism. There are significant correlations between VEN population and social interaction score ($p = 0.0143$) **(A)** and between pyramidal neuron population and restrictive and repetitive behavior score ($p = 0.0249$) **(B)** on the ADI-R.

In the only other quantitative neuropathologic study of this area in autism, Simms et al (19) reported that a subset of patients with autism had significantly smaller pyramidal neurons in layer V of the aMCC. This finding is consistent with previously reported reductions in pyramidal neuron size in the fusiform gyrus and in areas 44 and 45 (69, 70). The amygdala and fusiform gyrus also have reduced neuron density in autism, as reported by Simms et al (19), van Kooten et al (70), and Schumann and Amaral (71). These alterations in pyramidal neuron size and density may represent areas in which neuronal development or circuitry has been specifically affected in autism; not all cortical regions show such alterations (70, 72).

The functional consequences of abnormal connectivity in the aMCC may be reflected behaviorally as a need for consistency of routine to cope with the difficulty of selecting an appropriate response in an uncertain situation. The overlap in fear and pain areas in the aMCC implies that this area is involved in avoidance behavior (7), which has been reported to be increased in patients with autism (73). In this regard, we assessed whether the tested parameters correlated with symptom severity in patients with autism. We found that children presenting with an increase in restrictive and repetitive behaviors also had an increased amount of pyramidal neurons in the aMCC (Fig. 6). If we speculate that some neurons in the aMCC play a role in the generation of restrictive and repetitive behaviors, then this positive correlation may suggest a neural basis for increased severity of this symptom in some patients with autism. As the number of available cases increases in the future, we will be able to determine whether this relationship holds true with a larger cohort and broader severity distribution.

VENs in the aMCC

The presence of VENs adds another layer of complexity to the aMCC. These large bipolar spindle-shaped neurons are present in the anterior portion of the cingulate gyrus (namely, the ACC and the MCC), but their numbers quickly decrease in the posterior MCC (23, 25). The probable role of VENs in social functioning has been proposed based on their expression of vasopressin 1a receptors, which are involved in social bonding (74), and their location in both the frontoinsular cortex and the ACC, which are areas involved in empathy and emotion (75, 76). A role for VENs in the aMCC could be related to their strong expression of both dopamine D3 receptors and serotonin 2b receptors (76). Dopamine D3 receptors are linked to the expectation of reward under uncertainty (77), which is correlated with the function of the aMCC in response selection during an uncertain situation. Serotonin 2b receptors, on the other hand, are associated with the anticipation of punishment (78), suggesting that VENs may be signaling forthcoming punishment or danger and possibly a ''gut'' feeling of potential aversive situations. These opposing functions suggest that VENs in the aMCC may contribute to the intuitive feeling that often drives quick decisions by assessing the likelihood of punishment versus reward in a situation of uncertainty (76).

In addition, we assessed whether VEN number was correlated with any specific symptom of autism, as measured through ADI-R subcategories. We observed that young children with autism had a significant correlation between social interaction score on the ADI-R and VEN numbers, indicating that children who are more impaired in reciprocal social interaction have an increased amount of VENs (Fig. 6). Interestingly, Simms et al (19) also reported that a subgroup of their cohort of patients with autism had increased VEN density. This may reflect a subgroup with higher severity of social interaction deficits; however, this study did not correlate VEN density with individual autism characteristics. Because the aMCC is reciprocally connected with subcortical areas, such as the amygdala (11, 42–50), and VENs may transmit information on our homeostatic bodily state (25, 28, 79, 80), one potential explanation for the correlation between higher VEN number and increased social impairment is that the abnormal VEN number may underlie heightened anxiety and avoidance behaviors. As for our original question regarding selective VEN disruption in autism, we did not find a difference in VEN number or density in patients with autism and in controls. However, this does not suggest that abnormalities do not exist in VENs in the aMCC in autism; future studies should expand to include more properties

of VENs, such as gene and protein expression patterns and cellular volume.

In conclusion, the results of this study suggest that young children with autism show neuron-specific neuropathologic changes in the aMCC, an area primarily involved in response selection. Although this area is not strongly linked to the social and emotional aspects of behavior, it is a crucial component of our ability to adapt in novel situations. As young children with autism are characterized by their inability to adjust and their strong propensity for routines, the aMCC is a prime candidate for potential dysfunction in autism. In fact, the reduction in pyramidal neuron size suggests that this area may not be receiving the appropriate input to assess an uncertain situation, and that it may not be appropriately able to modulate areas involved in motor function to carry out an adequate response. This impairment in connectivity supports the hypothesis that patients with autism have global underconnectivity and local overconnectivity (81), which have been supported by many neuropathologic studies of autism (19, 69–71, 79, 82, 83). In addition, our data also suggest that the individual severity of autism in a young child may, in part, be tied to the severity of neuropathology. The correlation between neuronal pathology and increased severity of specific autism symptoms provides newfound insight toward potential cellular underpinnings of autism heterogeneity. These results, along with other neuropathologic findings in autism, suggest that the impact of autism occurs very early in life, likely in the prenatal period (69–72, 82, 83). In addition, the specificity of pyramidal neuron volume neuropathology in young children with autism corresponds to previous reports of distinct abnormalities in children that are not present in adults (81). The abnormalities characterized in postmortem cases are likely the compensatory effects of earlier insults, which may be much less pronounced with age, as indicated by the lack of abnormalities in adolescents with autism. These results provide a stronger understanding of cellular-level changes that may cause the behavioral changes in children with autism and provide insight on potential targets for early intervention.

ACKNOWLEDGMENTS

We thank Drs Jane Picket and Daniel Lightfoot (Autism Speaks), Mrs Ellen Xiu (Autism Speaks), and Dr Jerzy Wegiel (New York State Institute for Basic Research) for their help in securing the precious postmortem brain materials used in this study. We would also like to acknowledge the Bronx James J. Peter VA Medical Center Brain Bank, Harvard Brain Tissue Resource Center, National Institute of Child Health and Human Development Brain Tissue Bank, New York State Institute for Basic Research in Developmental Disabilities, Oxford Brain Bank, University of Maryland Brain and Tissue Bank, and University of Würzburg Morphologic Brain Research Unit for the materials used in this study. We are deeply indebted to the patients' families who have made this study possible.

REFERENCES

1. Center for Disease Control and Prevention. Prevalence of autism spectrum disorder among children aged 8 years—Autism and Developmental Disabilities Monitoring Network, 11 Sites, United States, 2010. MMWR Surv Summ 2014;63:1–21
2. Betancur C. Etiological heterogeneity in autism spectrum disorders: More than 100 genetic and genomic disorders and still counting. Brain Res 2011;1380:42–77
3. Allen G, Courchesne E. Attention function and dysfunction in autism. Front Biosci 2001;6:105–19
4. Bush G, Luu P, Posner MI. Cognitive and emotional influences in anterior cingulate cortex. Trends Cogn Sci 2000;4:215–22
5. Devinsky O, Morrell MJ, Vogt BA. Contributions of anterior cingulate cortex to behaviour. Brain 1995;118:279–306
6. Vogt BA, Finch DM, Olson CR. Functional heterogeneity in cingulate cortex: The anterior executive and posterior evaluative regions. Cereb Cortex 1992;2:435–43
7. Vogt BA, Berger GR, Derbyshire SW. Structural and functional dichotomy of human midcingulate cortex. Eur J Neurosci 2003;18:3134–44
8. Vogt BA, Hof PR, Vogt LJ. Cingulate gyrus. In: Paxinos G, Mai JK, eds. *The Human Nervous System*. San Diego, CA: Academic Press, 2004;915–49
9. Vogt BA, Vogt LJ, Nimchinsky EA, et al. Primate cingulate cortex chemoarchitecture and its disruption in Alzheimer's diesase. In: Bloom FE, Björklund A, Hökfelt T, eds. *The Primate Nervous System: Part I. Handbook of Chemical Neuroanatomy*, Vol. 13. San Diego, CA: Elsevier, 1997:455–28
10. Van Hoesen GW, Morecraft RJ, Vogt BA. Neurobiology of cingulate cortex and limbic thalamus: A comprehensive handbook. In: Vogt BA, Gabriel M, eds. *Connections of the Monkey Cingulate Cortex*. Boston, MA: Birkhauser, 1993:1265–77
11. Vogt BA, Pandya DN. Cingulate cortex of the rhesus monkey: II. Cortical afferents. J Comp Neurol 1987;262:271–89
12. Fan J, Hof PR, Guise KG, et al. The functional integration of the anterior cingulate cortex during conflict processing. Cereb Cortex 2008;18:796–805
13. Schmitz N, Rubia K, van Amelsvoort T, et al. Neural correlates of reward in autism. Br J Psychiatry 2008;192:19–24
14. Barnea-Goraly N, Kwon H, Menon V, et al. White matter structure in autism: Preliminary evidence from diffusion tensor imaging. Biol Psychiatry 2004;55:323–26
15. Fan J, Bernardi S, Van Dam NT, et al. Functional deficits of the attentional networks in autism. Brain Behav 2012;2:647–60
16. Haznedar MM, Buchsbaum MS, Wei TC, et al. Limbic circuitry in patients with autism spectrum disorders studied with positron emission tomography and magnetic resonance imaging. Am J Psychiatry 2000;157:1994–2001
17. Kemper TL, Bauman ML. The contribution of neuropathologic studies to the understanding of autism. Neurol Clin 1993;11:175–87
18. Vogt BA, Nimchinsky EA, Vogt LJ, et al. Human cingulate cortex: Surface features, flat maps, and cytoarchitecture. J Comp Neurol 1995;359:490–506
19. Simms ML, Kemper TL, Timbie CM, et al. The anterior cingulate cortex in autism: Heterogeneity of qualitative and quantitative cytoarchitectonic features suggests possible subgroups. Acta Neuropathol 2009;118:673–84
20. Heinsen H, Heinsen YL. Serial thick, frozen, gallocyanin stained sections of human central nervous system. J Histotechnol 1991;14:167–73
21. Heinsen H, Arzberger T, Schmitz C. Celloidin mounting (embedding without infiltration)—a new, simple and reliable method for producing serial sections of high thickness through complete human brains and its application to stereological and immunohistochemical investigations. J Chem Neuroanat 2000;20:49–59
22. Wegiel J, Kuchna I, Nowicki K ,et al. The neuropathology of autism: Defects of neurogenesis and neuronal migration, and dysplastic changes. Acta Neuropathol 2010;119:755–70
23. Nimchinsky EA, Vogt BA, Morrison JH, et al. Spindle neurons of the human anterior cingulate cortex. J Comp Neurol 1995;355:27–37
24. Brodmann K. *Vergleichende Lokalisationslehre der Grosshirnrinde in ihren Prinzipien dargestellt auf Grund des Zellenbaues*. Leipzig, Germany: Johann Ambrosius Barth, 1909
25. von Economo C. Eine neue Art Spezialzellen des Lobus cinguli and Lobus insulae. Zschr ges Neurol Psychiatr 1926;100:706–12
26. Schmitz C, Hof PR. Design-based stereology in neuroscience. Neuroscience 2005;130:813–31
27. West MJ, Slomianka L, Gundersen HJ. Unbiased stereological estimation of the total number of neurons in the subdivisions of the rat hippocampus using the optical fractionator. Anat Rec 1991;231:482–97
28. Butti C, Santos M, Uppal N, et al. Von Economo neurons: Clinical and evolutionary perspectives. Cortex 2013;49:312–26

29. Butti C, Sherwood CC, Hakeem AY, et al. Total number and volume of Von Economo neurons in the cerebral cortex of cetaceans. J Comp Neurol 2009;515:243–59
30. Hof PR, Van der Gucht E. Structure of the cerebral cortex of the humpback whale, *Megaptera novaeangliae* (Cetacea, Mysticeti, Balaenopteridae). Anat Rec 2007;290:1–31
31. Nimchinsky EA, Gilissen E, Allman JM, et al. A neuronal morphologic type unique to humans and great apes. Proc Natl Acad Sci U S A 1999; 96:5268–73
32. Gundersen HJ. The nucleator. J Microsc 1988;151:3–21
33. Chua P, Krams M, Toni I, et al. A functional anatomy of anticipatory anxiety. Neuroimage 1999;9:563–71
34. Hsieh JC, Stone-Elander S, Ingvar M. Anticipatory coping of pain expressed in the human anterior cingulate cortex: A positron emission tomography study. Neurosci Lett 1999;262:61–64
35. Porro CA, Baraldi P, Pagnoni G, et al. Does anticipation of pain affect cortical nociceptive systems? J Neurosci 2002;22:3206–14
36. Rushworth MF, Behrens TE. Choice, uncertainty and value in prefrontal and cingulate cortex. Nat Neurosci 2008;11:389–97
37. Sawamoto N, Honda M, Okada T, et al. Expectation of pain enhances responses to nonpainful somatosensory stimulation in the anterior cingulate cortex and parietal operculum/posterior insula: An event-related functional magnetic resonance imaging study. J Neurosci 2000;20:7438–45
38. Shackman AJ, Salomons TV, Slagter HA, et al. The integration of negative affect, pain and cognitive control in the cingulate cortex. Nat Rev Neurosci 2011;12:154–67
39. Vogt BA. Pain and emotion interactions in subregions of the cingulate gyrus. Nat Rev Neurosci 2005;6:533–44
40. Wallis JD, Kennerley SW. Heterogeneous reward signals in prefrontal cortex. Curr Opin Neurobiol 2010;20:191–98
41. Yu R, Zhou W, Zhou X. Rapid processing of both reward probability and reward uncertainty in the human anterior cingulate cortex. PLoS One 2011;6:e29633
42. Cauda F, D'Agata F, Sacco K, et al. Functional connectivity of the insula in the resting brain. Neuroimage 2011;55:8–23
43. Dum RP, Levinthal DJ, Strick PL. The spinothalamic system targets motor and sensory areas in the cerebral cortex of monkeys. J Neurosci 2009;29:14223–35
44. Ghashghaei HT, Hilgetag CC, Barbas H. Sequence of information processing for emotions based on the anatomic dialogue between prefrontal cortex and amygdala. Neuroimage 2007;34:905–23
45. Hatanaka N, Tokuno H, Hamada I, et al. Thalamocortical and intracortical connections of monkey cingulate motor areas. J Comp Neurol 2003;462: 121–38
46. Kunishio K, Haber SN. Primate cingulostriatal projection: Limbic striatal versus sensorimotor striatal input. J Comp Neurol 1994;350:337–56
47. Mesulam MM, Mufson EJ. Insula of the old world monkey: III. Efferent cortical output and comments on function. J Comp Neurol 1982;212:38–52
48. Morecraft RJ, McNeal DW, Stilwell-Morecraft KS, et al. Amygdala interconnections with the cingulate motor cortex in the rhesus monkey. J Comp Neurol 2007;500:134–65
49. Roy AK, Shehzad Z, Margulies DS, et al. Functional connectivity of the human amygdala using resting state fMRI. Neuroimage 2009;45:614–26
50. Yu C, Zhou Y, Liu Y, et al. Functional segregation of the human cingulate cortex is confirmed by functional connectivity based neuroanatomical parcellation. Neuroimage 2011;54:2571–81
51. Bush G, Vogt BA, Holmes J, et al. Dorsal anterior cingulate cortex: A role in reward-based decision making. Proc Natl Acad Sci U S A 2002;99: 523–28
52. Gu X, Gao Z, Wang X, et al. Anterior insular cortex is necessary for empathetic pain perception. Brain 2012;135:2726–35
53. Shima K, Tanji J. Role for cingulate motor area cells in voluntary movement selection based on reward. Science 1998;282:1335–38
54. Adolphs R. What does the amygdala contribute to social cognition? Ann N Y Acad Sci 2010;1191:42–61
55. LeDoux J. The amygdala. Curr Biol 2007;17:868–74
56. Kanner L. Autistic disturbances of affective contact. Nerv Child 1943; 2:217–50
57. American Psychiatric Association. *Diagnostic and Statistical Manual of Mental Disorders 5*. Washington, DC: American Psychiatric Publishing, 2013
58. Fan J, Van Dam NT, Gu X, et al. Quantitative characterization of functional anatomical contributions to cognitive control under uncertainty. J Cogn Neurosci 2014;26:1490–506
59. Gilbert CD, Kelly JP. The projections of cells in different layers of the cat's visual cortex. J Comp Neurol 1975;163:81–105
60. Hayes TL, Lewis DA. Hemispheric differences in layer III pyramidal neurons of the anterior language area. Arch Neurol 1993;50:501–5
61. Jacobs B, Driscoll L, Schall M. Life-span dendritic and spine changes in areas 10 and 18 of human cortex: A quantitative Golgi study. J Comp Neurol 1997;386:661–80
62. Lund JS, Lund RD, Hendrickson AE, et al. The origin of efferent pathways from the primary visual cortex, area 17, of the macaque monkey as shown by retrograde transport of horseradish peroxidase. J Comp Neurol 1975;164:287–303
63. Amatrudo JM, Weaver CM, Crimins JL, et al. Influence of highly distinctive structural properties on the excitability of pyramidal neurons in monkey visual and prefrontal cortices. J Neurosci 2012;32:13644–60
64. Kabaso D, Coskren PJ, Henry BI, et al. The electrotonic structure of pyramidal neurons contributing to prefrontal cortical circuits in macaque monkeys is significantly altered in aging. Cereb Cortex 2009;19:2248–68
65. Luebke JI, Medalla M, Amatrudo JA, et al. Age-related changes to layer 3 pyramidal cells in the rhesus monkey visual cortex. Cereb Cortex [published online ahead of print December 8, 2013; DOI: 10.1093/cercor/bht336]
66. Lee JE, Bigler ED, Alexander AL, et al. Diffusion tensor imaging of white matter in the superior temporal gyrus and temporal stem in autism. Neurosci Lett 2007;424:127–32
67. Waiter GD, Williams JH, Murray AD, et al. Structural white matter deficits in high-functioning individuals with autistic spectrum disorder: A voxel-based investigation. Neuroimage 2005;24:455–61
68. Petanjek Z, Judas M, Simic G, et al. Extraordinary neoteny of synaptic spines in the human prefrontal cortex. Proc Natl Acad Sci U S A 2011; 108:13281–86
69. Jacot-Descombes S, Uppal N, Wicinski B, et al. Decreased pyramidal neuron size in Brodmann areas 44 and 45 in patients with autism. Acta Neuropathol 2012;124:67–79
70. van Kooten IA, Palmen SJ, von Cappeln P, et al. Neurons in the fusiform gyrus are fewer and smaller in autism. Brain 2008;131:987–99
71. Schumann CM, Amaral DG. Stereological analysis of amygdala neuron number in autism. J Neurosci 2006;26:7674–79
72. Uppal N, Gianatiempo I, Wicinski B, et al. Neuropathology of the posteroinferior occipitotemporal gyrus in children with autism. Mol Autism 2014;5:17
73. Chamberlain PD, Rodgers J, Crowley MJ, et al. A potentiated startle study of uncertainty and contextual anxiety in adolescents diagnosed with autism spectrum disorder. Mol Autism 2013;4:31
74. Insel TR, Young LJ. The neurobiology of attachment. Nat Rev Neurosci 2001;2:129–36
75. Allman JM, Tetreault NA, Hakeem AY, et al. The von Economo neurons in frontoinsular and anterior cingulate cortex in great apes and humans. Brain Struct Funct 2010;214:495–517
76. Allman JM, Watson KK, Tetreault NA, et al. Intuition and autism: A possible role for Von Economo neurons. Trends Cogn Sci 2005;9:367–73
77. Sokoloff P, Guillin O, Diaz J, et al. Brain-derived neurotrophic factor controls dopamine D3 receptor expression: Implications for neurodevelopmental psychiatric disorders. Neurotox Res 2002;4:671–78
78. Deakin JF, Graeff FG. 5-HT and mechanisms of defence. J Psychopharmacol 1991;5:305–15
79. Santos M, Uppal N, Butti C, et al. von Economo neurons in autism: A stereologic study of the frontoinsular cortex in children. Brain Res 2011; 1380:206–17
80. Seeley WW, Merckle FT, Gaus SE, et al. Distinctive neurons of the anterior cingulate and frontoinsular cortex: A historical perspective. Cereb Cortex 2012;22:245–50
81. Courchesne E, Pierce K. Why the frontal cortex in autism might be talking only to itself: Local over-connectivity but long-distance disconnection. Curr Opin Neurobiol 2005;15:225–30
82. Courchesne E, Mouton PR, Calhoun ME, et al. Neuron number and size in prefrontal cortex of children with autism. JAMA 2011;306:2001–10
83. Stoner R, Chow ML, Boyle MP, et al. Patches of disorganization in the neocortex of children with autism. N Engl J Med 2014;370:1209–19

